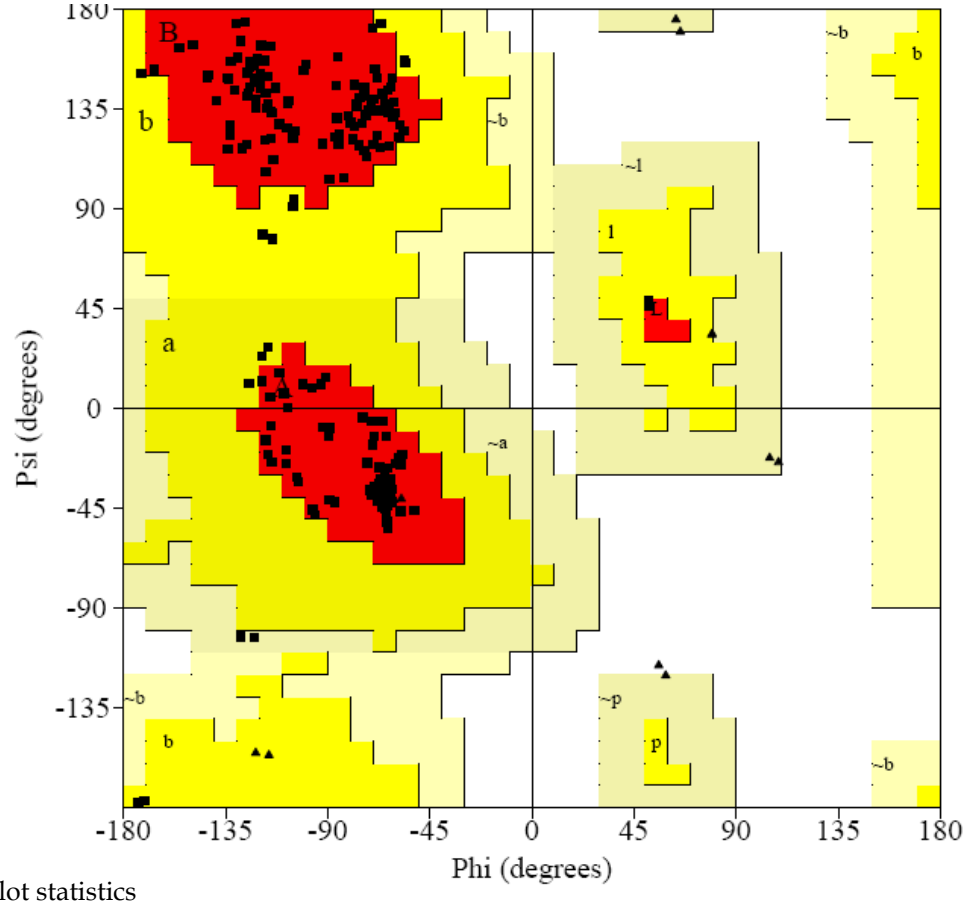

Figure S1: Ramachandran Plot of the predicted model of PemK of *Bacillus anthracis*: This figure is generated by PROCHECK. The red regions in the graph indicate the most allowed regions whereas the yellow regions represent allowed regions. Glycine is represented by triangles and other residues are represented by squares.

Plot statistics

Residues in most favoured regions [A,B,L]	193	92.8%
Residues in additional allowed regions [a,b,l,p]	13	6.2%
Residues in generously allowed regions [~a,~b,~l,~p]	2	1.0%
Residues in disallowed regions	0	0.0%
	----	------
Number of non-glycine and non-proline residues	208	100.0%
Number of end-residues (excl. Gly and Pro)	4	
Number of glycine residues (shown as triangles)	12	
Number of proline residues	8	

Total number of residues	232	

Based on an analysis of 118 structures of resolution of at least 2.0 Angstroms and R-factor no greater than 20%, a good quality model would be expected to have over 90% in the most favored regions.

Figure S1.

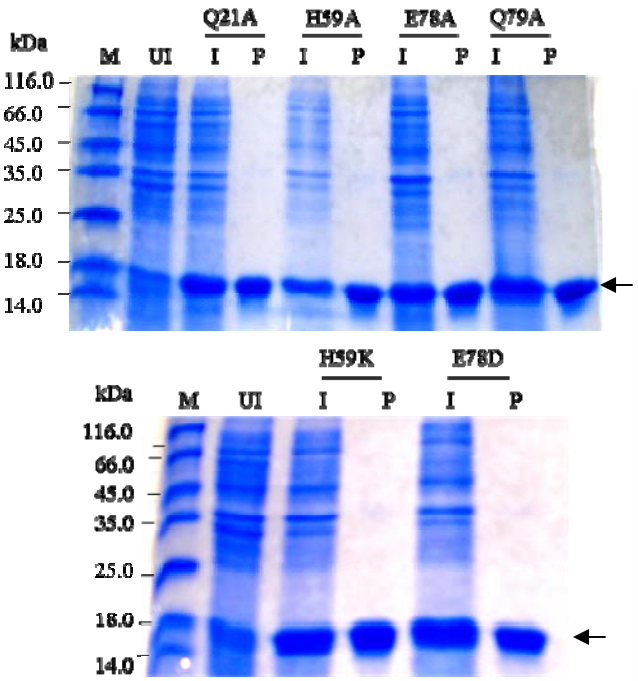

Figure S2.

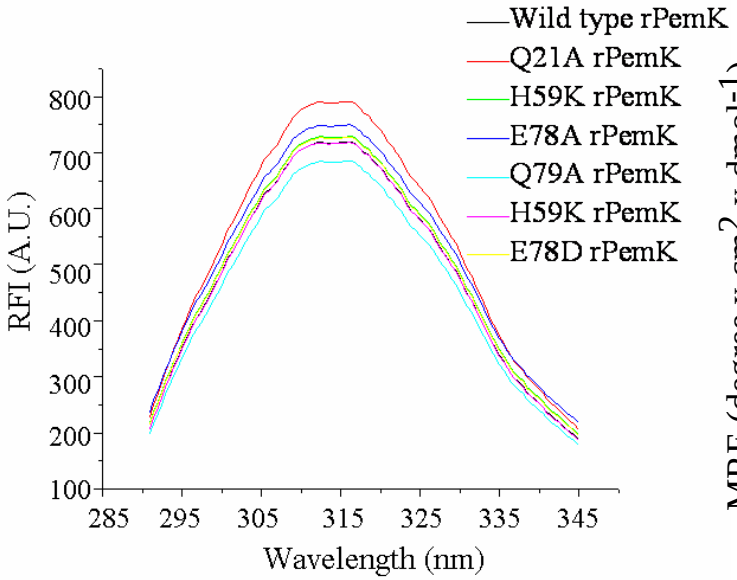

Figure S3.

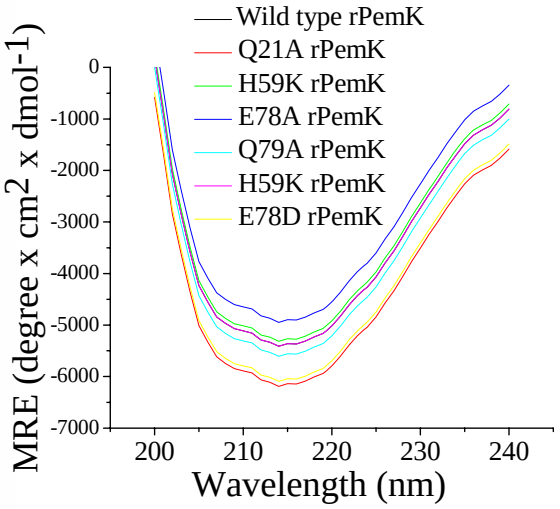

Figure S4.

Figure S2: Expression and purification of site specific mutants of the rPemK: Commassie blue-stained 12 % SDS-PAG; Lanes I represent the crude cell lysates obtained post induction with 1 mM IPTG for 4 h at 37 °C for the mutants of the rPemK as indicated on the top of the gel; Q21A.rPemK, H59A**.**rPemK, E78A.rPemK, Q79A.rPemK, H59K.rPemK and E78D.rPemK; Lane UI depicts the crude lysate harvested before induction; Lanes P represent the corresponding recombinant proteins purified from the soluble fraction employing Ni^{+2}-NTA affinity chromatography. The migration of protein molecular mass standards is shown in Lane M and the arrow points towards the purified recombinant protein.

Figure S3: Fluorescence spectroscopy of the rPemK (wild type) and mutants: Fluorescence emission maxima in each case was obtained at 25 °C in 10 mM potassium phosphate buffer, pH 8.0 at a concentration of 0.5 mg/ml. Emission spectrum was obtained by exciting the samples at 280 nm (slit width 20 nm) and monitoring the emissions from 295 nm to 350 nm (slit width 20 nm).

Figure S4: CD spectroscopy of the rPemK (wild type) and mutants: CD spectra of the rPemK and its mutants (0.1 mg in 10 mM phosphate buffer saline, pH 7.4) were obtained using Jasco Corp., J-815 spectropolarimeter at 25 °C using a 1 mm cell, wavelengths between 200 and 250 nm and at a scanning speed of 20 nm/min. The CD signals were converted to molar ellipticity by the following relationship: Φm = Φo x 100/lc, where Φm is molar ellipticity (in degrees per square centimeter per decimole), Φo is the observed ellipticity (in degrees), l is the path length (in centimeters), and c is the molar concentration.

Figure S5.

Sequence	Length	MW	pI	GRAVY	Solubility	% activity
VERLVSGG (Peptide I)	8	816	5.97	0.325	Partially insoluble	11
NLHRNIW (Peptide II)	7	952	9.76	-1.043	S	20
LLFQHLTE (Peptide III)	8	1000	5.47	0.412	S	35
KRYQHESM (Peptide IV)	8	1078	8.60	-2.35	S	25
RRGYIEMG (Peptide V)	8	980	8.75	-1.025	Partially insoluble	30
KAELVNDI (Peptide VI)	8	900	4.37	-0.013	S	22
LLKKIPKDVLEIYSE (NSP-15)	15	1780	6.30	-0.087	S	0
MSESSVTT (NTP-8)	8	841	4.00	-0.150	S	0

Figure S5: The physico-chemical parameters of the experimental (Peptide I-Peptide VI) and control (NSP-15 and NTP-8) peptides, deduced employing ProtParam at Expasy (www.expasy.ch).

Figure S6

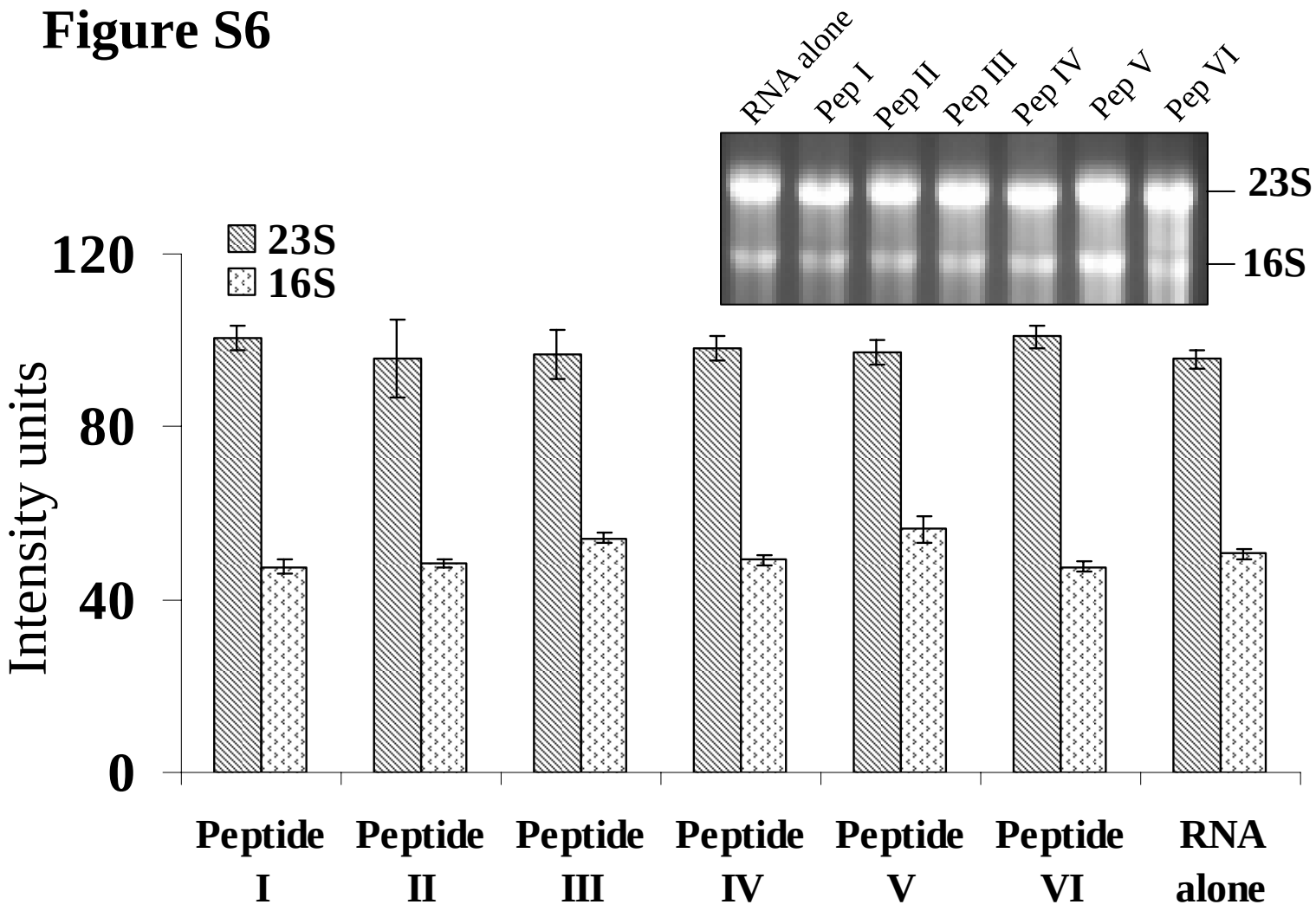

Figure S6: Peptides alone have no effect on RNA degradation: RNA (5 μg) was incubated with 2 μM of the indicated peptides (X- axis) for 2 h at 37 °C and were analyzed on 1.5 % formaldehyde gel (inset). The intensities of both the 23S and 16S bands were quantitated using the Bio-Rad densitometeric software and plotted. The bars represent mean ± SD.

Figure S7.

Figure S7: Superposition of toxin (PemK) and MazF and critical sites of interaction between MazE and MazF with catalytic residues. The model generated for PemK was superimposed on the MazF dimer. The two monomers of the MazF are shown in cyan and green while MazE is shown in orange. The ribbon of PemK dimer is shown in black. The two most critical sites of interaction (labeled Site1 and Site2) between MazE and MazF in the crystal structure are shown. W73 of MazE in Site1 is shown. Residues 66-73 (blue) of MazE bind to Site1 while 55-62 (yellow) bind to site2. These were used to propose peptide II and VI, respectively. The catalytic residues, H59 and E78, are shown in red sticks. The figure rendering was done with Pymol (Delano Scientific).

Figure S8.

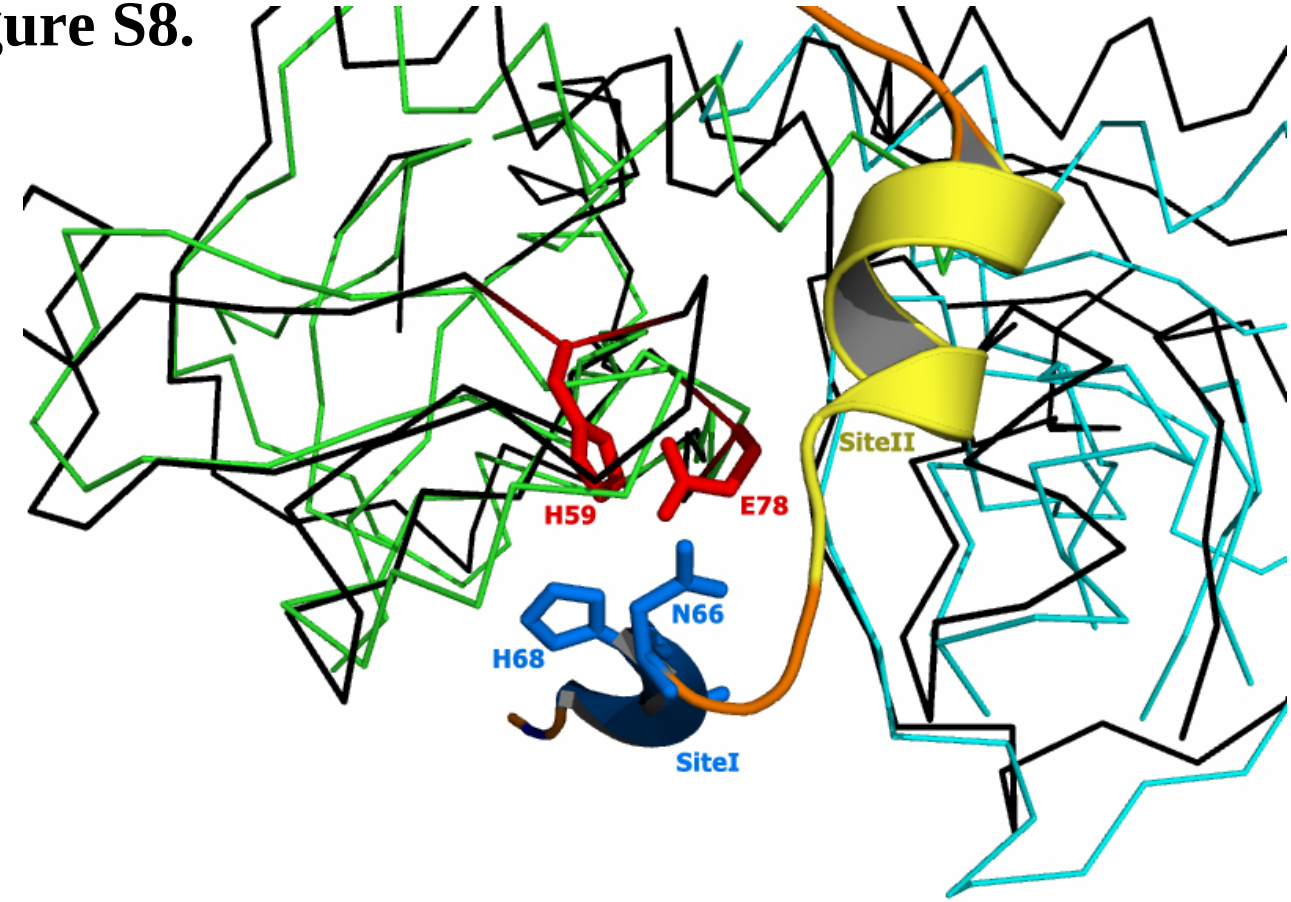

Fig. S8: Interaction of PemK catalytic residues (H59 and E78) with antitoxin, MazE. Close view of the contacts made by the catalytic residues of toxin, H59 and E78, with residues of the MazE antitoxin. E78 of PemK makes contact with H68 of MazE while H59 of PemK makes contact with both H68 and N66 of MazE, although H68 and N66 are located in the Site1 (Shown in blue sticks). The figure was drawn using Pymol.

Figure S9.

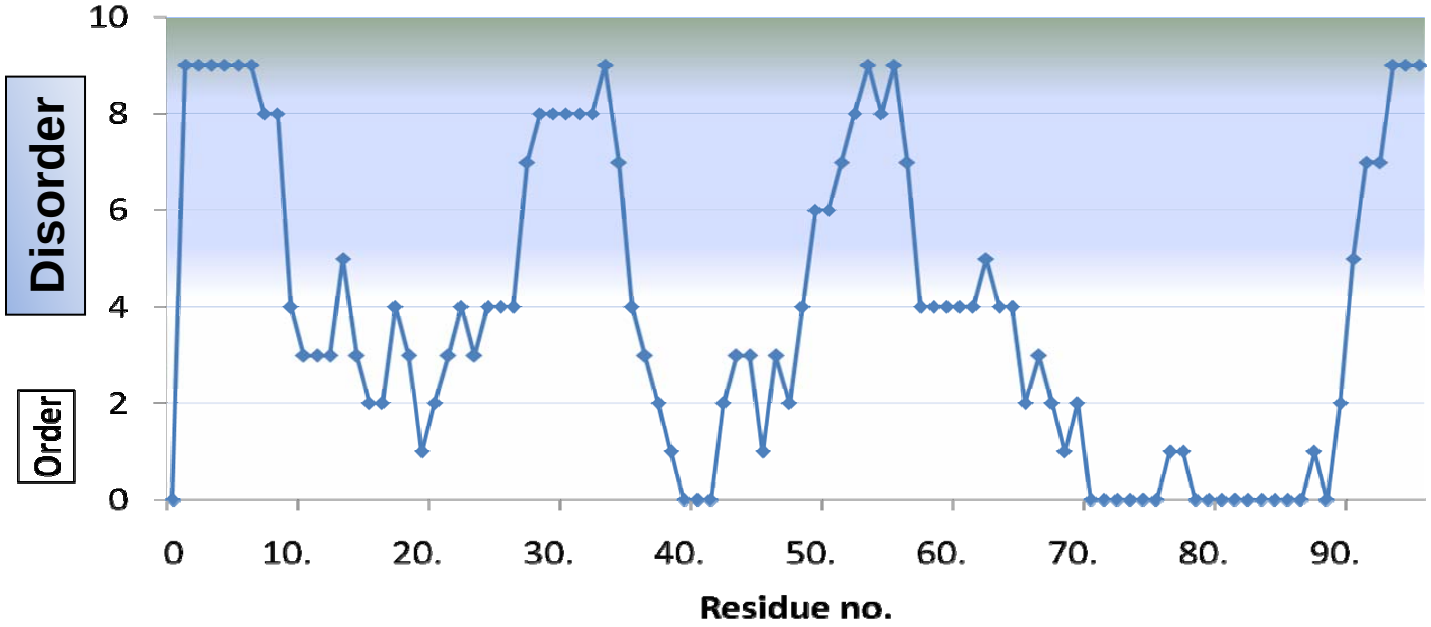

Figure S9: Phyre prediction for disorder probability of residues of PemI. The residues at N-terminus, C-terminus and in two intervening regions, comprising 33 % of the total residues, have high probability of being disordered